Lund University

Chaos for science and technology

FMFN05/FYST13

Chaotic Epidemiology

Authors:
Jonas Petersson
Elias H. Aronsson

Supervisor:
Andrea Idini

June 14, 2020

1 Introduction

The dangers of global disease spread have been highlighted this year with the COVID-19 outbreak. It is therefore of great interest to model such outbreaks and study their dynamics. In this project this is what we have done. The stability and dynamics of different compartment models for disease spread, as well as a cellular automata and a detailed balance travel implementation of spatial spread will be explored.

2 Background

2.1 SIR Model

One of the most basic models for simulating the spread of a disease is the SIR-model. In this model you start with a susceptible population (S) that will become infected (I) and then either develop immunity or die, both of which will count as removed (R) from the rest of the population. By adding a birth rate (B) and a death rate (μ), it is also possible to include what is called vital dynamics which enables a steady stream of new susceptible people. It is common to set $B = \mu$ in order to keep the population constant over time, they can also be put to zero for a more simple model. A condition that often is imposed is also that $N = S + I + R$ which ensures that the population stays constant over time. [1]

$$\frac{dS}{dt} = BN - \beta\frac{SI}{N} - \mu S \tag{1}$$

$$\frac{dI}{dt} = \beta\frac{SI}{N} - \gamma I - \mu I \tag{2}$$

$$\frac{dR}{dt} = \gamma I - \mu R \tag{3}$$

2.2 Cellular automata

The model discussed previously approximates the population as one whole with no differences in constants or initial conditions depending on spatial position. To capture the spatial spread and variations a cellular automata can be used. These are systems where both the time and state variables are discrete[2]. To represent 2-dimensional spread a 2d grid can be used. The interactions across the grid depends on a rule which defines the state in a cell in the next time step depending on the states in neighbouring cells and how this neighbourhood is defined.

2.3 SEIR Model

The basic SIR-model can be extended with one more population group, the exposed (E). This makes it possible to capture the behaviour of diseases that have an incubation time, and the effect is that there will be latency of the growth of the outbreak compared to the basic SIR-model. Also in this model it is common to use the constrain $N = S + E + I + R$.

$$\frac{dS}{dt} = BN - \beta\frac{SI}{N} - \mu S \tag{4}$$

$$\frac{dE}{dt} = \beta\frac{SI}{N} - \sigma E - \mu E \tag{5}$$

$$\frac{dI}{dt} = \sigma E - \gamma I - \mu I \tag{6}$$

$$\frac{dR}{dt} = \gamma I - \mu R \tag{7}$$

2.4 Seasonal Variation

Something that can be observed in diseases is that the infectivity varies with the seasons. Commonly the infectivity is the highest in the coldest time of the year when people spend more time in closed spaced and less in the warmer time of the year when people spend more time outdoors. This can be included in the infectivity parameter (β) as seen in eq. 8.

$$\beta = \beta_0(1 + \beta_1 cos(2\pi t)) \tag{8}$$

2.5 SEIR Model With Spatial Movement

One way of extending the SEIR-model to include spatial spread is by creating a travel matrix ω and having M cells with separate populations. By making ω symmetric it will ensure that the population in each cell stays constant while making it possible to simulate people leaving the cell and entering the cell from other cells.

$$\frac{dS_i}{dt} = BN_i - \beta\frac{S_i I_i}{N_i} - \mu S_i + \sum_{i \neq j} \omega_{j,i} S_j - \omega_{i,j} S_i \tag{9}$$

$$\frac{dE_i}{dt} = \beta\frac{S_i I_i}{N_i} - \sigma E_i - \mu E_i + \sum_{i \neq j} \omega_{j,i} E_j - \omega_{i,j} E_i \tag{10}$$

$$\frac{dI_i}{dt} = \sigma E_i - \gamma I_i - \mu I_i + \sum_{i \neq j} \omega_{j,i} I_j - \omega_{i,j} I_i \tag{11}$$

$$\frac{dR_i}{dt} = \gamma I_i - \mu R_i + \sum_{i \neq j} \omega_{j,i} R_j - \omega_{i,j} R_i \tag{12}$$

3 Results

To get a feel for the models the they were first run with some common parameters. Figures 1 to 3 shows the plotted time series of the results, both with a single cell and a 10 by 10 grid. Here the proximity infection model, described in section 5.1.1, was used.

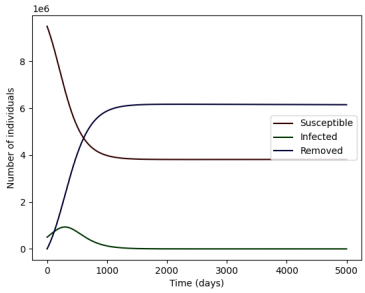

(a) Single spatial cell.

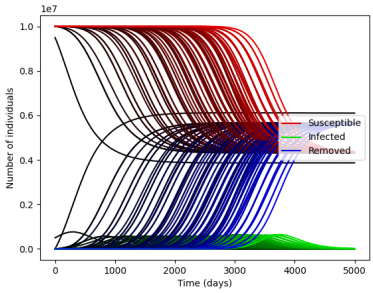

(b) 10 by 10 spatial cell grid, and initially one cell infected in the left upper coroner. $m = 0.005$.

Figure 1: SIR-model with parameters, $\beta = 0.25$, $\gamma = 0.2$, $B = 0.000032$, $\mu = 0.000025$, $N = 10000000$ *and* $I(0) = 0.05 \cdot N$.

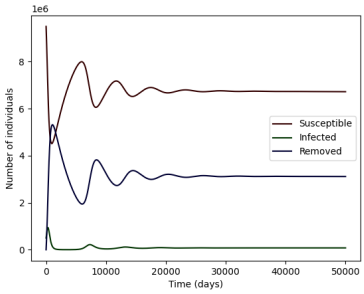

(a) Single spatial cell.

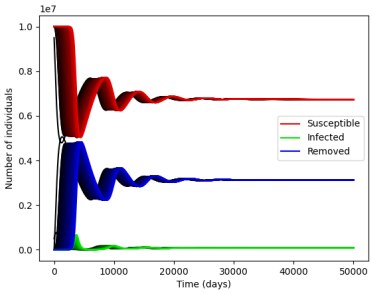

(b) 10 by 10 spatial cell grid, and initially one cell infected in the left upper coroner. $m = 0.005$.

Figure 2: SIR-model with seasonal forcing and parameters, $\beta_0 = 2$, $\beta_1 = 0.25$, $\gamma = 0.2$, $B = 0.000032$, $\mu = 0.000025$, $N = 10000000$ *and* $I(0) = 0.05 \cdot N$.

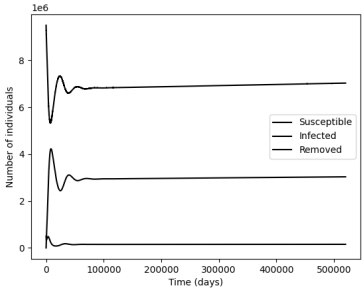

(a) Single spatial cell.

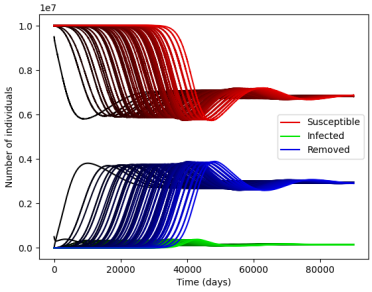

(b) 10 by 10 spatial cell grid, and initially one cell infected in the left upper coroner. $m = 0.005$.

Figure 3: SEIR-model with seasonal forcing and parameters, $\beta_0 = 2$, $\beta_1 = 0.25$, $\gamma = 0.2$, $B = 0.000032$, $\mu = 0.000025$, $\sigma = 0.2$ $N = 10000000$ *and* $I(0) = 0.05 \cdot N$.

3.1 SEIR-Model With Seasonal Variation

Parameter	β_0	γ	σ	μ	B
Value	1800	100	35.48	0.02	0.02

Table 1: Parameters used for SEIR-Model with seasonal variations that has been found in another paper [3].

The first thing we did to get an overview of the behaviour of the model while using eq. 4-7 was to use the parameters in table 1 while varying the strength of the seasonality (β_1) from eq. 8. We observe two regions with chaotic behaviour, firstly with β_1 roughly between 0.2-0.58 and secondly with β_1 roughly between 0.65-0.85, this can be seen in figure 4.

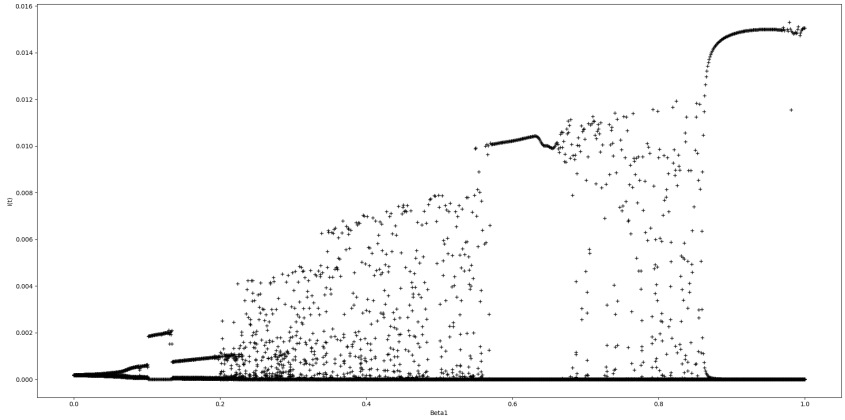

Figure 4: Simulations were run with 10 different initial conditions for each β_1 (x-axis). The first half of the simulated time series data is discarded and for the second half the minimums and maximums are plotted. This yields a plot similar to a bifurcation diagram where one can identify chaotic parameter values.

When looking at a time series plot with β_1 in the chaotic region it is observed that simulations with slightly different initial conditions behave very similarly in the beginning to later on diverge, which is typical of chaotic systems, this can be seen in figure 5.

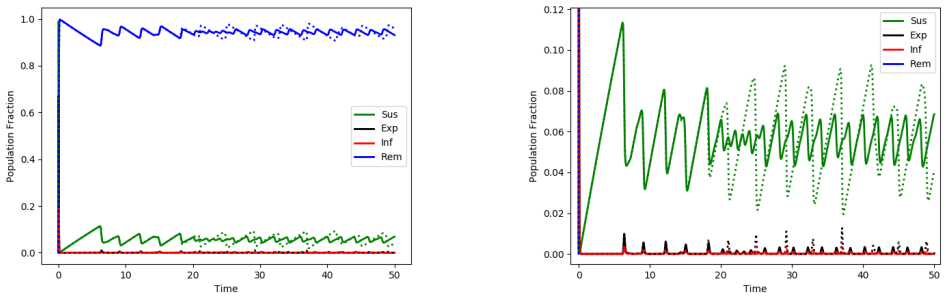

(a) Full plot

(b) Zoomed plot

Figure 5: SEIR-model with seasonal variation, $\beta_1 = 0.28$. The chaotic behaviour becomes obvious around $t = 20$

To further investigate the behaviour in the different regions of β_1 seen in figure 4 the susceptible population is plotted against the infected population for 3 simulations with different initial conditions as seen in figure 6. It is clear that if there is no seasonality dependence, the simulation converges to a fixed point. When $\beta_1 = 0.175$ it is instead visible that the paths are more complicated, but they still converging to the same limit cycle, something that also is seen for $beta_1 = 0.62$. In the chaotic region, $\beta_1 = 0.28$, the initially similar paths quickly diverge as expected for if the system is chaotic.

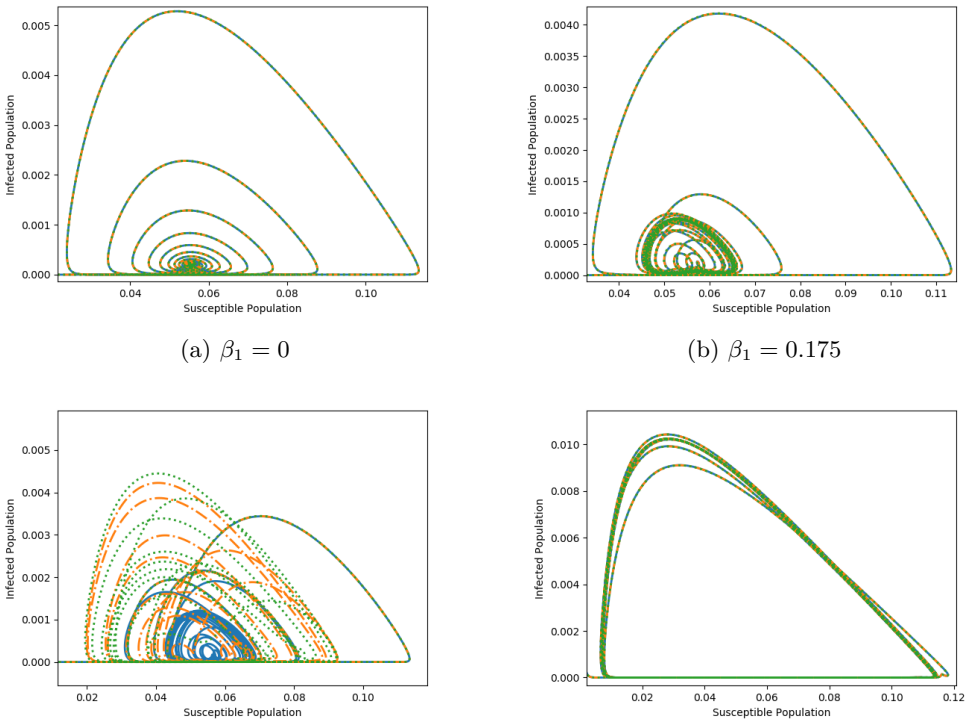

(a) $\beta_1 = 0$

(b) $\beta_1 = 0.175$

(c) $\beta_1 = 0.28$

(d) $\beta_1 = 0.62$

Figure 6: Three simulations are plotted with the initial fraction of infected being 0.01,0.0105, and 0.011. Chaotic behaviour can be seen in ***(c)****.*

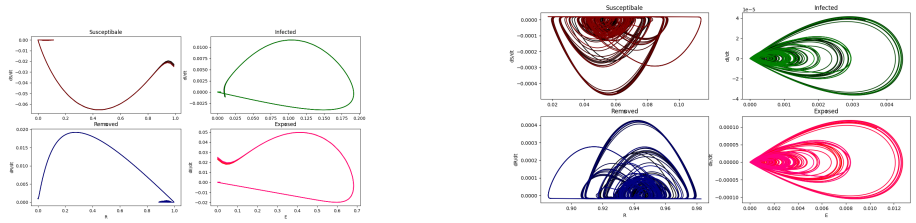

(a) Full plot

(b) Iterations 1000 to 8000.

Figure 7: Graph of the number of individuals in the different compartments plotted against their corresponding time derivatives, for four simulations with initially infected from 0.01 to 0.011.

3.2 Spatial SEIR-Model With Seasonal Variation

In order to investigate how the model can be translated into a spatial system of cells with inhomogeneous population, Sweden's regions are chosen as a starting point, read more in section 5.1.2.

A new behaviour can be observed in this spatial model, which is clear when $\beta_1 = 0.62$, see fig 8 c), d), e). Although the initial trajectories are following each other, two initial conditions leads to two different oscillatory patterns that does not seem to converge over long periods of time.

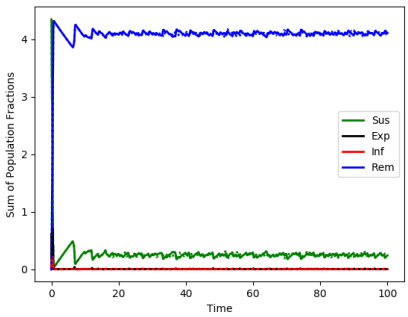

(a) $\beta_1 = 0.28$

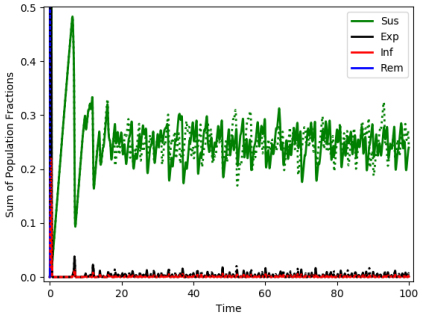

(b) $\beta_1 = 0.28$

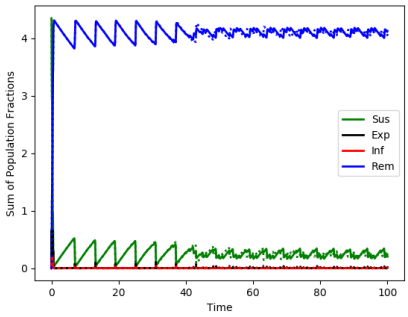

(c) $\beta_1 = 0.62$

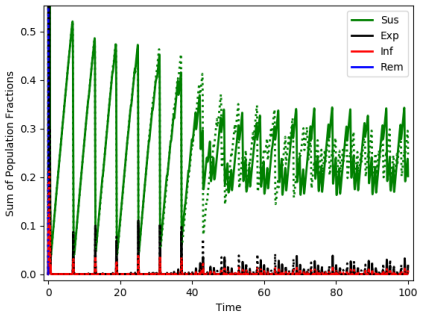

(d) $\beta_1 = 0.62$

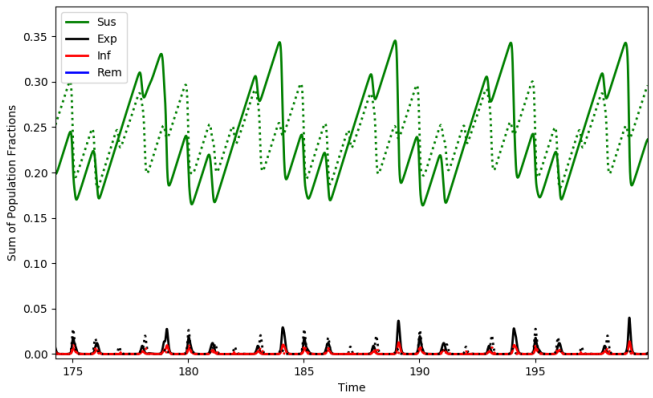

(e) $\beta_1 = 0.62$, long time

Figure 8: Spatial SEIR-model with seasonal variation. Two simulations are plotted with the initial fraction of infected in Stockholm being $5 \cdot 10^{-6}$ *and* 10^{-5}*, respectively corresponding to the solid and the dashed line.*

Just as in the non-spatial model, dissipative motion towards a fixed point can be observed when there is no seasonal forcing, compare figure 6 a) and 9 a). Continuing to compare figure 6 and 9 it also becomes clear that there is a different behaviour for the non-chaotic value of β_1. Although the system becomes more sensitive to initial conditions it does not seem to become chaotic, rather, different initial conditions seems to put the system in different periodic orbits which likely are governed by the travel matrix (ω) and the populations of the cells.

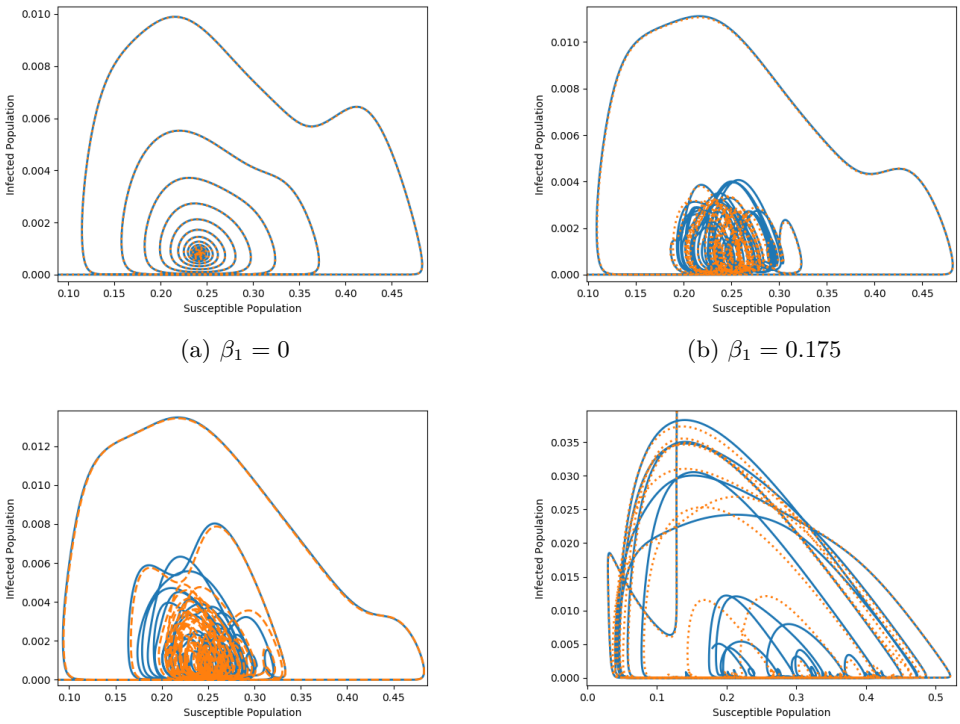

(a) $\beta_1 = 0$

(b) $\beta_1 = 0.175$

(c) $\beta_1 = 0.28$

(d) $\beta_1 = 0.62$

Figure 9: Two simulations are plotted with the initial fraction of infected in Stockholm being $5 \cdot 10^{-6}$ *and* 10^{-5}*. The only case where the trajectories follow each other closely is if* $\beta_1 = 0$*.*

3.3 Parameter Sensitivity

To see how sensitive the system is to changes in different parameters a number of different simulations were run for 50000 time steps and the final 10 values plotted against the value of the tested parameter. The SEIR-model with seasonal forcing was used. The non varying parameters were set according to table 1. 255 simulations were run for every parameter sweep, except m when only 36 runs were simulated due to the computation time. When assessing the sensitivity of the system to changes in m a six by six grid was used along with the proximity infection model, while only a single cell was used for the other parameters.

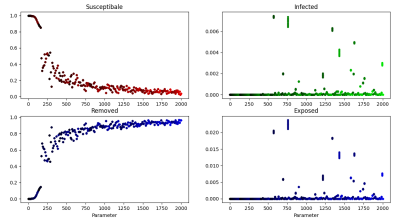

(a) β varying from 0 to 2000.

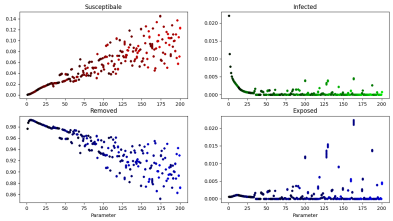

(b) γ varying from 0 to 200.

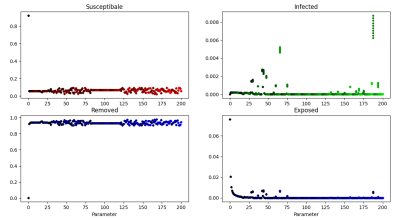

(c) σ varying from 0 to 200.

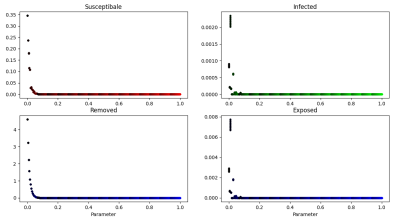

(d) μ varying from 0 to 1.

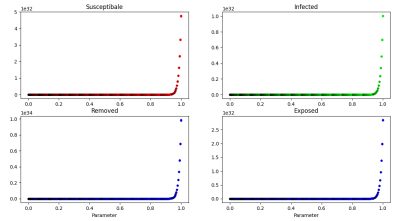

(e) B varying from 0 to 1.

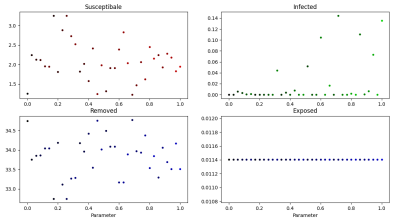

(f) m varying from 0 to 0.9999.

Figure 10: Final 10 values for simulations with different different parameters plotted against the parameter.

It is also interesting to look at how the size of the time step affects the simulations. As can be seen in figure 11 the simulation shows high sensitivity to small differences. Both time steps with sizes in the order of 10^{-2}, as seen in figure 11a and 10^{-3}, as seen in figure 11b show this sensitivity. They do display the same behavior initially thought, and the paths starts to diverge at about the same time. Running simulations with time step one order of magnitude lager than this results in the values going towards infinity. Simulations with time steps one order of magnitude smaller than this results in extended computation times.

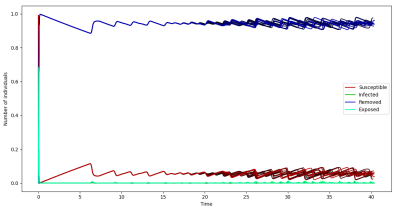

(a) Time step varying from 0.001 to 0.00101, while run for 4000 iterations.

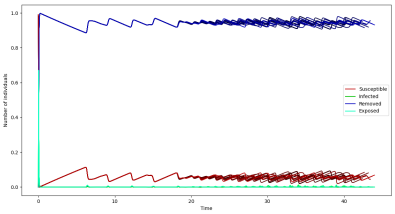

(b) Time step varying from 0.0001 to 0.0011, while run for 40000 iterations.

Figure 11: Time series for simulations with varying size of time step.

4 Conclusions

We have seen that it is possible to simulate the spread of a disease with different models of varying complexity. In a SEIR-model with seasonal variations of the infectivity, the chaotic behaviour becomes obvious. If the model is extended to include spatial spreading, certain parameters yields fixed oscillatory patterns that change depending on the initial conditions. It would be of interest to further study how these patterns change depending on population size in different spatial cells, as well as the transmission rate between cells, number of cells, and which between which cells travel is allowed. Understanding how recurring outbreaks might behave differently over time depending on the localization and size of the initial outbreak might be of interest in the field of computational epidemiology since the world is likely to face more diseases as cities grow denser and international travel expands further.

An interesting result is the stability of the models. Even with seasonal forcing the chaotic regions lie in narrow bands in several of the parameters. The models are of course limited compared to the complexity of real disease spread, but it might still have some implications for the predictability of such events.

The high sensitivity to the size of the time step is a big limiting factor in the models. The resulting need for this to be very small yields lengthy computation times and a more advanced numerical method would be an interesting improvement. A natural improvement would be to use a higher order Runge-Kutta method instead of the explicit Euler method as well as higher precision floats such as quadruple or octuple precision floats.

5 Method

A framework to solve and analyze the models described in section two was implemented using the explicit Euler method in python.

5.1 Spatial Models

5.1.1 Proximity Infection

For each population compartment a 3-dimensional array is constructed, where one axis represent time and the other two x- and y-position respectively. The value in each cell represents the number of individuals in that, time, place and population group.

Using the Euler formula the progression in time is calculated. For each time step a 2-dimensional convolution of the matrix of infected and a square matrix set to zero in the center surrounded by ones, is taken. Using the same logic as for disease spread in the original models a parameter m is added. This is meant to represent the probability of infection multiplied by the mean number of contacts in a neighbouring cell. Now the value in each position in the convolution matrix multiplied with the number of susceptible individuals at the corresponding index in the susceptible matrix multiplied with this constant, m, represents the number of new infections form neighboring cells. For SIR and a three by three window the model becomes;

$$\frac{dS}{dt} = BN_{i,j} - \beta\frac{S_{i,j}I_{i,j}}{N_{i,j}} - \mu S_{i,j} - \frac{m}{N_{i,j}}\left(\left(\sum_{n=i-1}^{i+1}\sum_{m=j-1}^{j+1} I_{n,m}\right) - I_{i,j}\right) \tag{13}$$

$$\frac{dI}{dt} = \beta\frac{SI}{N} - \gamma I - \mu I + \frac{m}{N_{i,j}}\left(\left(\sum_{n=i-1}^{i+1}\sum_{m=j-1}^{j+1} I_{n,m}\right) - I_{i,j}\right) \tag{14}$$

$$\frac{dR}{dt} = \gamma I - \mu R \tag{15}$$

but this extra factor of infection from the neighbouring cells can be added to any of the models.

5.1.2 Traveling Matrix

For the simulation equation 9-12 is used with the parameters in table 1. To construct the travel matrix the regions of Sweden were indexed and by looking at a map, a list was created for each region which contained the indices of it's neighbours. The travel matrix then becomes a symmetric sparse matrix with a 1 for neighbours and 0 otherwise, the matrix is the scaled down by 10^7 to slow down the rate of travel.

Further, the population of each region was divided by the the region with the highest population (Stockholm) in order to avoid large numbers. For all the plots the sum of all the regions are then plotted.

References

[1] Jianhong Wu Fred Brauer Pauline van den Driessche. *Mathematical Epidemiology*. Springer, 2008.
[2] Per Östborn Gunnar Ohlén Sven Åberg. *Chaos*. Lund University, 2007.
[3] Na Yi et al. "Analysis and control of an SEIR epidemic system with nonlinear transmission rate". In: *Mathematical and computer modelling* 50.9-10 (2009), pp. 1498–1513.